Optimization and Validation of Solar Pump Performance by MATLAB Simulink and RSM

Singh, Vineet
Department of Mechanical Engineering, School of Engineering and Technology, IFTM University

Vinod Singh Yadav
National Institute Technology, Srinagar, India. Department of Mechanical Engineering

Kumar, Manoj
Department of Mechanical Engineering, School of Engineering and Technology, IFTM University

Kumar, Niraj
Department of Mechanical Engineering, School of Engineering & Technology, IIMT University

https://doi.org/10.5109/6625723

出版情報：Evergreen. 9 (4), pp.1110-1125, 2022-12. 九州大学グリーンテクノロジー研究教育センター
バージョン：

Optimization and Validation of Solar Pump Performance by MATLAB Simulink and RSM

Vineet Singh[1*], Vinod Singh Yadav[2,] Manoj Kumar[3,] Niraj Kumar[4]

[1,3]Department of Mechanical Engineering, School of Engineering and Technology, IFTM University, Moradabad, Uttar Pradesh, India.

[2]National Institute Technology, Srinagar, India. Department of Mechanical Engineering, Uttarakhand, India.

[4]Department of Mechanical Engineering, School of Engineering & Technology, IIMT University, Meerut, Uttar Pradesh, India

*Author to whom correspondence should be addressed:
E-mail: vineet.singh@iftmuniversity.ac.in

(Received October 10, 2022; Revised November 4, 2022; accepted November 5, 2022).

Abstract: In this paper, a 335 W solar panel with a centrifugal pump combined system was simulated in MATLAB Simulink 2018 with fuzzy logic-based MPPT, and the voltage, current, power, and discharge four output responses were determined at different values of solar flux, module temperature, and atmospheric temperature. Further, the output responses voltage, current, power output, and discharge data have been optimized in Response Surface Methodology (RSM). The output data of RSM and MATLAB Simulink is used to determine the solar pump's theoretical performance and overall efficiency. Finally, the RSM-optimized results of solar pumps are validated with the experimental results of the solar pump. The experimental setup consists of 15 panels of 335 W power and a 5 hp submersible pump operated by an AC motor. The experimental data were collected from 15/01/2020 to 15/12/2020. The optimization of the solar pump by the three most important variables solar flux, module temperature, and the atmosphere temperature is very new and unique since the selected input variables maximize the overall performance of the solar pump.

Keywords: Photovoltaic; Submersible pump; Discharge; Head; Exegetic efficiency; Temperature.

1. Introduction

In India, agriculture depends on monsoons, canals, tanks, wells, tube wells, and other sources of irrigation. The tube wells contribute 63.63% of irrigation compared to other available irrigation sources in India. In India, the tube wells are run by electricity and diesel fuels. In recent times, the price of fossil fuels has increased. The enlarged cost of fossil fuels incurred the high cost of irrigation in agriculture charged by the farmers reducing their earnings of the farmer. If solar pumps operated by PV modules are used for the irrigation of crops, it not only reduces the cost of irrigation but also works as a source of earning for the farmers after the payback period. If the cost of the Solar Photovoltaic (SPV) system is around ten lacs, that will return in 4 years of payback. However, the actual life of the pump is 20 years. It will also increase farmers' earnings by three lacs per year [1)].

The statistical analysis covers the long-term performance of the solar pumps. The statistical equation in the form of a regression equation has been generated by the motor pump manufacturer and weather data. Based on these models, the solar pump system performance has to be determined for future use. The simulation study has been done by the TRYNS model and validated the results with the UW-PUMP program. The percentage difference between simulation and experimental results was 3% in Albuquerque and 6% in Seattle [2)].

The investigation was performed on rice and unrice crops under drip and furrow irrigation in Bangladesh. Finally, it is concluded that a solar pump is not suitable for rice because it requires three times more water than other crops [3)]. A compressive review was presented on PV and organic Rankine cycle-operated solar pumps. The focus area chosen for the study was the sub-Sahara region. Finally, it is concluded that for small size capacity solar pump thermal energy-operated solar pump is not suitable [4)].

A review paper in 108 reputed journals has been presented on a solar pump. The research focused on finding the research gap, economic feasibility, design variables, performance, and atmospheric effects on PV

cell technology. They also focused on the material of PV cells, optimized performance, and degradation of PV modules [5]. A solar pump has been installed at St. Catherine, South Sinai, Egypt, climate. The pump consists of 4 modules of PV cells made of the silicon monocrystalline of module size 0.8x1.6m^2, which generated the short circuit current (Isc= 5.65A) and open-circuit voltage (Vo= 0.617 V). The simulation model of solar flux, PV cell has been solved by MATLAB and a graph has been plotted between solar intensity to time at different seasons of the years. The graphs were plotted for 21 June, 21 march, and 21 Dec, between solar radiation in W/m2 and time from 5 am to 7 pm. He finally concluded that solar radiation is maxing at 21 June 920 W/m^2. The tilt angle has been changed as (L-15) on 21 June, L on 21 march, and (L+15) on 21 Dec, where L represents the latitude of the location [6].

A directly- coupled PV water pumping system performance has to be determined based on the experimental finding. A 1.5 kWp solar pump with a centrifugal pump has been installed, the system consists of 30 PV modules, of which 15 modules were in series in one row, and both rows were parallel to each other. The total power, voltage, and current produced by the PV array were 1526.07 W, 253.5 V, and 6.04 A respectively [7]. A nonlinear mathematical formulation between solar power and water flow rate has been developed by mathematical regression analysis. The formulation was done at varying heads in which eight series and three parallel PV modules were used. The experimental setup used for the formulation was located in the Madinah site (Saudi Arabia) [8].

A PV-operated solar pump was designed and developed for pumping the water to fill the domestic need of Purwodadi village, Tepus in the karsts of Gunungkidul. The two pumps are designed for pumping water from 250 m head. A total of 32 solar panels were used for supplying 3200 Wp power to the motor for supplying the water at varying flow rates from 0.4- 0.9 LPM [9]. The solar panel arrangement determines the performance of the solar pump. The various arrangement of solar pumps has been studied in [10].

They measured the effect of different arrangements on solar panel efficiency, the overall efficiency of the solar pump system, and the field of irrigation of different types of crops. The four varieties of crops chosen are wheat, potato, tomato, and sunflower. A solar pump was designed and developed for the desert area of Jordan. They have used 56 panels, 14 in series, and four parallel combinations. The total power developed by solar panels was 2800 W with 230 V DC (Direct Current). The mathematical model has been designed and numerically solved to find the solar pump's performance parameters [11].

A new approach to optimization had to be developed in which objective function was formulated by considering the initial cost of investment, revenue cost, and availability of solar energy, and the head of the groundwater level was considered as the constrained. The sensitivity study shows the effect of the total cost of crop and the total cost of the photovoltaic module on the objective function [12]. The simulation results on the different case studies are also performed on the solar pump by putting MPPT and VRFB**.** They also conclude that pump performance parameters like output power and solar panel efficiency have fluctuated without VRFB when the system directly coupled to MPPT [13].

A different approach of optimization has been used in which the head developed by the pump is maximized based on input energy supplied by the solar panel. The model has been validated in two locations in Croatia one was Split, and the other was Osijel [14]. The economic feasibility of the PV water pump and diesel engine is checked in [15]**.** The comparison between different capacity solar water pumps and the diesel engine size varies from 2.8 kW to 15 kW. The sensitivity of the systems to be proved at different location and different conditions of the enviroment. The solar pumping system have been installed in Faculty of Engineering and Technology (FET) **.** The study was conducted for comparing the solar water pumping system and existing system rum by conventional energy source. The total cost of SPV system is around 10 lac that will return in 4 year of payback. However the life of the pump was twenty years then it supplied the water upto sixteen years without spending the any cost [16]. A large scale study was conducted on the solar pump in eight states of Mexico in which 130 types of solar pump analyses of varying ranges from small power to 2 Kwp. The manufacturer data have been used for financial study of PV operated solar pump with the traditionally used methods of irrigation [17]. A comparative study of solar pumps and diesel engines was conducted to determine economic savings annually. The author also found a reduction in CO_2 emission and cost due to the installation of the solar photovoltaic pump in India. The author also summarized the data between solar flux and the cost of diesel fuel according that if daily solar flux supplies are around 5.5 kWh/m^2 for 1.8 kWp solar photovoltaic pump US 405.06/ton cost saving [18]. Solar tracking is an essential part of the solar panel, it will maximize the solar flux striking at the surface of solar panel. The tracking can be installed for one axis and two axis but the cost of two axis tracking is high. A study was conducted on south India in tamil Nadu at a village by installing a both axis tracking system. For study a hybrid optimization multiple energy resource (HOMER) software was used for analying power geneation capacity of solar pump for supplying the water and electricity for village [19].

A literature review on previous articles shows that the tilt, surface azimuth angle of PV module, solar flux, PV module temperature, atmospheric temperature, discharge, and head of the pump are the input parameters on which the performance of solar pump depends. The pump discharge, head developed depends on the input energy received by the submersible pump. The energy

received by the submersible pump depends on the solar flux, PV module cell temperature, and atmosphere temperature. So in this research paper Response Surface Methodology (RSM) tool is used to determine the optimum setting of input parameters on which solar panel will produce the maximum power. In the previous article, no optimization techniques were used to optimize the solar pumps' performance based on the MATLAB Simulink technique and RSM simultaneously.

2. Model used for solar panel electrical circuit I-V and P-V characteristic graph

The calculating the performance characteristic of the PV module, it is necessary to draw its equivalent circuit. The circuit is drawn on MATLAB SIMULINK software. The input parameters, the temperature of solar cell material, solar flux intensity, and atmospheric temperature, affect the power output of solar panels as shown in Figure 1.

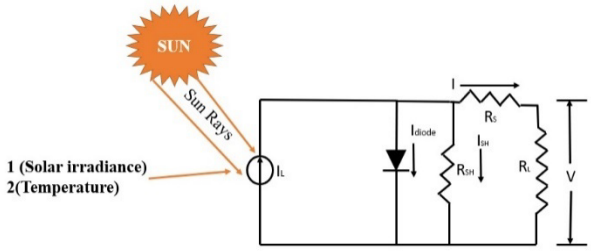

Fig. 1: solar cell equivalent circuit

In this circuit, points (1,2) represent the (irradiance and temperature) for the two main input parameters in the solar panel. The circuit measured the current, voltage, and power output at the different input parameters.

The circuit consists of a diode current I_{diode}, series resistance Rs, photocurrent I_L, I_{SH} is a shunt, and I is current at the output end (load current). Now by Kirchhoff's law

$$I_L = I + I_{diode} + I_{SH} \quad (1)$$

$$I = I_L - I_{diode} - I_{SH} \quad (2)$$

Where I_{diode}, I_{SH} is the diode current and shunt current given by [20] book **of Photovoltaic system engineering**.

$$I_{diode} = I_O(e^{(\frac{ev}{KT})} - 1) \quad (3)$$

$$I = I_L - I_O(e^{(\frac{ev}{KT})} - 1) - \frac{(V + IR_S)}{R_{SH}} \quad (4)$$

Where Io is the reverse saturation current represented in terms of the open-circuit voltage in [9].

$$I_O = I_L e^{(\frac{ev_{OC}}{KT})} \quad (5)$$

Where V_{oc} is the OCV, K is the BC, and T is the MT.

2.1 PV module Simulink model drawing on MATLAB 2018

Figure 2 represents the solar panel MPPT with fuzzy logic combined with a centrifugal pump illustrated in MATLAB Simulink. The solar power output depends on the solar flux and the temperature of the solar panel. The current and voltage model equations represented by equations (3) and (4) show the temperature dependence. These model equations are nonlinear and have three unknowns (I_L, I, V), so difficult to solve. As shown in Figure 4, the simulation model requires two inputs and displays the output parameters in the shortest time. The Solar panel connects the two inputs and three outputs. The Simulink circuit has been drawn in MATLAB by connecting the series resistance, capacitor, inductance, diode, relay, memory block fuzzy logic tool, centrifugal pump, tank, resistive pipe, etc. The final output power has to be determined by using a multiplier in the circuit that connects the voltage and current. The total power produced by PV modules connected to the DC motor is connected by field and armature winding with the voltage source, the same voltage applied at the power source generated by the PV module. The power output from the DC motor in the form of torque is connected to the centrifugal pump. Finally, the centrifugal pump is connected to the reservoir, and the tank between a resistive pipe is connected.

2.2 Fuzzy logic control

The fuzzy logic theory is used for making a decision at a time of uncertainty. It is proposed first time as the fuzzy set theory by the scientist Lotfi Zadeh. This model can handle, represent, manipulate and interpret very vague and uncertain data [21]. Fuzzy concepts have applicability in many fields like artificial intelligence and control systems. The fuzzy rule is applied as per the block diagram illustrated in Figure 3. The main objective behind the use of Fuzzy Logic (FLC) is to optimize the power at the PV modules output so that solar pump discharge and head developed increased [22].

The logic (Algorithm) behind the working of fuzzy logic is demonstrated in the block diagram represented in Figure 3. The method 1st provides the duty ratio, now calculates the power output, and determines the error in the nth and (n-1) duty cycles. The change in error is also determined to improve the algorithm's effectiveness. The fuzzy system has provided the error and change in error data, which work as the input of the fuzzification. The fuzzification data and fuzzy rule represented in Table 1 work as information to the interface of the fuzzy tool. It will give the change in duty ratio and compare it with the actual value. This algorithm effectively calculates the maximum power point on the P-V curve.

2.3 Fuzzification

Fuzzification is the method to provide the numerical values of the membership function in the range of 0 to 1.

If its value is zero, it does not belong to the fuzzy set, and 1 belongs entirely to the fuzzy set. The fuzzy set is defined in triangular and trapezoidal shapes, the maximum value of the slope is 1 and decreases toward zero. Figure 4 defines the MF of the input and output variable

The five MF define the fuzzy rule in inputs and output variables. Each membership function is determined by the fuzzy rule illustrated in Table 1. The fuzzy rule sets shown in Table 1 are defined as Negative Big (NB), Negative Small (NS), ZE (zero), Positive Small (PS), and Positive Big (PB). The MF of the triangular symmetric shape has been selected for fuzzification, as shown in Figure 4.

Table 1: Fuzzy Rule followed

ΔV_{PV} @[O/P}	ΔV_{PV} [I/P}					
ΔP_{PV} [I/P}		NB	NS	ZE	PS	PB
	NB	PS	PB	NB	NS	NS
	NS	PS	PS	NS	NS	NS
	ZE	ZE	ZE	ZE	ZE	ZE
	PS	NS	NS	PS	PS	PS
	PB	NS	NB	PB	PS	PS

2.4 Defuzzification

Defuzzification is a process in which it takes the output from the fuzzy set in the form of actual value. It converts the fuzzy controller output into numerical values. In the defuzzification, the center of gravity of the triangle lies on the abscissa and is used for the selection of duty ratio. The change in duty ratio has been defined by the following equation represented in [22].

$$\Delta D = (\sum_{i=1}^{i=n} \mu_i x_i S_i \Delta D_i)/(\sum_{i=1}^{i=n} \mu_i S_i \Delta D_i) \qquad (7)$$

Where n is the number of fuzzy sets, μ_i is the weight of the center of gravity at i_{th} subset, x_i is the abscissa of the triangle, and the S_i is the surface of the triangle. The final duty ratio is the previous duty ratio plus the change in duty ratio in the last value, as illustrated in Figure 3. The MF of input and output variables is given in Figure 4. Every MF must be defined by the fuzzy rule represented in Table 1. The input and output variables are selected in range, and the total number of points in the selected range is 181.

3. Optimization Methods

The optimization techniques are used for finding the optimum value of solar flux, solar cell material temperature, and atmospheric temperature at which the performance of solar panels is maximum. The output data of current, voltage, and power have to be generated by MATLAB Simulink circuit revealed in Figure 4 at the corresponding values of SF varies from 400, 700, 1000 W/m^2, solar cell temperature varies from 20, 50, 80°C and atmospheric temperature varies from 25, 35, 45°C. Finally, output response parameters current, voltage, power output, and discharge are optimized by RSM in MINITAB 17 software. The RSM is the mathematical tool used for solving mathematical equations by statistical techniques performing the regression analysis, and fitting the data in two-degree nonlinear polynomial equations. The RSM form the relation among the several input variables and one and more RV. This method was first time used by George E P Box and KB Wilson in 1951. The RSM generates a matrix that has a sequence of experimental data on which response has been collected and analyzed. The matrix was formed in the DOE (Design of Experiment) based on input factors. The number of experimental runs depends on the selected model and the total number of factors. In this problem, Behnken Box Design (BBD) 3 factorial approach is used, which shows 15 runs. As shown in Table 2.

Analysis of Variance (ANOVA) is used in the RSM for the regression analysis. The F and P values determine the effectiveness of the model. The F value is the ratio of the mean sum of squares due to treatment to the mean sum of squares due to error. The P-value is the probability of fit data representing the confidence level, if the confidence level is 95%, it deleted the values higher than the alpha value of 0.05. The higher F value and lower P-value represent the level of accuracy of ANOVA. The results of the ANOVA model have been given in Table 3.

Table 2 Total 15 runs with the input and response parameters

S. N.	Solar Flux (W/m^2)	Module Temperature (°C)	Atmospheric Temperature (°C)	Voltage(V)	Current (I)	Power (P)	Discharge (Q)
1	1000	50	45	520	8.46	4400	12
2	700	80	25	440	6.81	3000	10
3	700	20	25	580	6.03	3500	11
4	400	50	45	520	2.88	1500	5
5	400	80	35	440	2.95	1300	3
6	1000	20	35	580	7.93	4600	12.5
7	700	80	45	440	6.59	2900	6
8	700	50	35	520	6.15	3200	10.5
9	400	50	25	520	2.88	1500	5.1
10	1000	80	35	580	6.89	4000	11.5

11	1000	50	25	520	8.46	4401	12.3
12	700	50	35	520	6.15	3201	10.51
13	700	50	35	520	6.15	3200	10.1
14	700	20	45	580	5.51	3200	10.2
15	400	20	35	520	8.46	4400	11.98

Table 3 and Table 4 show the statical analysis of the regression equation generated by the ANOVA, it is an inherent property of ANOVA that it deleted the values of p greater than the reference value at the time of regression analysis due to the inbuilt null hypothesis. The 2nd-order polynomial equation has been generated by the ANOVA regression analysis in RSM by MINITAB 17 software. The response parameters are represented as the 2nd-order polynomial equations in terms of input parameters SF, solar cell temperature, and AT. The equations are represented as follows.

Table 3. Effectiveness coefficients of ANOVA model for current and voltage

		Current (I)				**Voltage (V)**			
Sources	DF	Adj. SS	Adj. MS	F-value	P-value	Adj. SS	Adj. MS	F-value	P-value
Model	9	22.22	2.46	2.39	0.175	268.81	29.86	2.41	0.172
Linear	3	18.9	6.31	6.12	0.040	227.78	75.92	6.14	0.040
It	1	15.9	15.9	15.44	0.011	191.297	191.27	15.46	0.011
MT	1	3.01	3.01	2.92	0.148	36.46	36.45	2.95	0.147
AT	1	0.00080	0.00080	0.01	0.933	0.018	0.018	0.00	0.971
Square	3	1.5762	0.5254	0.51	0.693	20.59	6.86	0.55	0.667
It*It	1	0.0175	0.0175	0.02	0.930	0.201	0.201	0.02	0.904
MT*MT	1	0.5698	0.5698	0.55	0.491	8.71	8.71	0.66	0.453
TA*TA	1	0.8682	0.8682	0.84	0.401	10.36	10.62	0.62	0.396
2-way Interaction	3	1.6872	0.5624	0.55	0.672	20.439	6.813	0.65	0.669
It*MT	1	1.6861	1.6861	1.63	0.257	20.439	20.83	1.55	0.255
It*AT	1	0.0004	0.0004	0.00	0.985	0.000	0.000	0.47	0.996
MT*AT	1	0.0007	0.0007	0.00	0.981	0.0008	0.0008	0.00	0.981
Error	5	5.1567	1.0375	-	-	61.84	12.37	0.00	-
Lack of Fit	3	0.0001	0.000	-	0.0000	61.82	20.608	-	0.0000
Pure Error	2	27	10.296	-	-	0.024	0.012	1698	-
Total	14	27.36	-	-	-	330.6	-	-	-

Table 4. Effectiveness coefficients of ANOVA model for power and discharge

		Current (I)				**Voltage (V)**			
Sources	DF	Adj. SS	Adj. MS	F-value	P-value	Adj. SS	Adj. MS	F-value	P-value
Model	9	30511	2.46	2.39	0.190	116.96	12.99	14.84	0.004
Linear	3	25970	6.31	5.79	0.044	49.84	16.61	18.97	0.004
It	1	2116	15.9	14.18	0.013	2.889	2.889	3.30	0.129
MT	1	4770	3.01	3.19	0.134	0.012	0.012	0.01	0.147
AT	1	3.5	0.00080	0.00	0.963	0.018	0.018	0.00	0.911
Square	3	2933	0.52554	0.65	0.614	2.905	2.905	2.32	0.128
It*It	1	808	0.01775	0.54	0.495	4.124	1.3741	1.57	0.307
MT*MT	1	873	0.5698	0.58	0.479	0.009	0.0088	0.01	0.924
TA*TA	1	1068	0.8682	0.72	0.436	0.068	0.0682	0.08	0.791
2-way Interaction	3	1607	0.5624	0.36	0.786	3.586	3.5858	4.09	0.099
It*M	1	160	1.68	1.0	0.3	3.9	1.3	1.5	0.3

T		6	61	8	74	31	501	0	23
It*AT	1	1.2	0.0004	0.00	0.978	0.083	0.0825	0.09	0.771
MT*AT	1	0.0	0.0007	0.00	0.996	0.008	0.008	0.00	0.981
Error	5	7471.5	1.0375	-	-	3.149	3.1485	3.59	0.116
Lack of Fit	3	7467.3	0.000	-	0.000	0.303	0.0302	-	0.000
Pure Error	2	4.2	10.296	-	-	0.019	0.017	32.67	-
Total	14	37982.7	-	-	-	302.6	-	-	-

$$I = 1.57 + 0.0002(q) - 0.1161(T_m) + 0.336(T_a) + 0.000001(q)^2 + 0.000436(T_m)^2 - 0.00485(T_a)^2 + 0.000072(q)(T_m) - 0.000003(q)(T_a) + 0.00004(T_m)(T_a) \quad (8)$$

$$V = 5.7 + 0.0000(q) - 0.418(T_m) + 1.17(T_a) + 0.000003(q)^2 + 0.00165(T_m)^2 - 0.0170(T_a)^2 + 0.000251(q)(T_m) - 0.000003(q)(T_a) + 0.00015(T_m)(T_a) \quad (9)$$

$$P = 23 + 0.163(q) - 4.09(T_m) + 12.0(T_a) + 0.000164(q)^2 + 0.0171(T_m)^2 - 0.0170(T_a)^2 + 0.00223(q)(T_m) - 0.00019(q)(T_a) + 0.0003(T_m)(T_a) \quad (10)$$

$$Q = -3.40 - 0.0135(q) - 0.223(T_m) + 1.049(T_a) + 0.000015(q)^2 + 0.00165(T_m)^2 - 0.0150(T_a)^2 + 0.000033(q)(T_m) - 0.000014(q)(Ta) + 0.00005(T_m)(T_a) \quad (11)$$

The effectiveness of the fitted curve has been checked by measuring the error between the modeled and experimental data provided. The R^2, S, and R^2(adj) are the three parameters used for measuring the errors in ANOVA analysis. The R^2 values for current (I), voltage (V), power, and discharge (Q) are respectively 81.16%, 81.30%, 80.33%, and 78.38%, which are greater than 75% higher than the considerable accepted limit. The S values for current, voltage, power, and discharge are 1.0555, 3.51708, 38.6561, and 2.44, respectively, and R^2(adj) values for the current, voltage, power, and discharge are 73.36%, 89.42%, 91.07%, and 88%. The R^2, S, and R2(adj) values show good accuracy, so these model equations can be generalized and used for finding the performance parameters of the solar panel at different values of input parameters. The P and F tests shown in Table represents the effectiveness of the ANOVA model. Now above explanation clearly shows that model is validated with 95% accuracy.

The Table 3 and Table 4 represents the values of terms like sources, DF, Adj. SS, Adj.MS. The sources represents the name of the variables like model, linear TA etc. The DF, Adj. SS and Adj. MS represents the degree of freedom, adjusted sumes of squares and Adjusted mean squares. The magnitude of thease terms represents the error of the ANOVA.

Figure 5 (a) and (b) display the effect of input variables SF, module temperature, and atmospheric temperature on responses in terms of standardized effect and error (residual) by Pareto chart and residual plot. Figure 5 (a) shows the overall standardized effect of all input variables on the response (Current) is 2.571. The standardized effect of solar flux, module temperature, and AT is 4, 2.7, and 0.2. It shows the effect of SF on the current is maximum for the other two input variables. The effect of AT is the least on the current. So, for producing the maximum power output, researchers focus on increasing the sola flux and reducing the module temperature without bothering about AT. Figure 5 (b) shows the residual plot between 15 observations. The residual is the difference between the RSM predicted results and data generated by the MATLAB Simulink software. So, residuals represent the error, sometimes, the residual may be positive and negative, but the sum of residuals for all observations is zero. The maximum residual is 1.0 for 15 observations and -1.0 for 10 observations.

4. Results and Discussions

4.1 MATLAB Simulink results

4.1.a Effect of solar cell temperature on the current, voltage, and power output

The overall performance of the PV solar water pump depends on the solar panel and motor pump system efficiency. The overall efficiency of the solar pump is less due to the poor performance of the solar panel at higher temperatures. Figures 6 (a) and (b) show the effect of solar cell temperature variation on the current, voltage, and power output of the solar panel [24], [25]. The total 15 PV module is connected in series in MATLAB Simulink, and the input solar flux was selected to be 1000 W/m^{2,} and solar cell temperature setting data varied from 20°C, 50°C, and 80°C. The Figure 6 (b) clearly shows that if solar cell temperature increases from 20 to 80°C, the power output is reduced from 4800 W to 3200 W since increased module temperature increases the resistivity of semiconductor material and also enhances the heat loss in the atmosphere by convection and radiation [26, 27], [28], [29], [30]. It can be seen from Figure 6 (a) that if the cell temperature increased from 20°C to 80°C the short circuit variation was negligible, even a little bit of increment seen in short circuit current due to increased temperature of solar cell material the same results also verified in [31]. The variation of cell temperature from 20°C to 80°C has an immense impact on the open-circuit voltage, it is reduced from 30 V to 20 V, as seen in Figures 6 (a), (b) [28], [31].

4.1.b Effect of solar flux on the current, voltage, and power output

Figure 7 (a) and (b) represent the impact of solar flux on the output responses. Figure 7 (a) shows that increased solar flux from 400 W/m^2 to 1000 W/m^2 enhanced the short circuit current from 5.5 to 9.1 amp but had a Negligible effect on open-circuit voltage [31]. Figure 7 (b) shows that if solar flux increased from 400 W/m^2 to 1000 W/m^2, the power output of the PV module enhanced from 2500 W to 4890 W.

5 Optimization Results

5.1 Variation of current with the input parameters

Figure 8 (a) illustrated the effect of solar flux, PV module temperature, and atmospheric temperature on the PV module output current generated. Figure 8 (a) shows that if the SF increases, the output current is continuously increased, but enhancement in module temperature reduces the output current since the increased temperature of the PV module increases the semiconductor material's resistivity [32]. Figure 8 (b) shows that if the atmospheric temperature is below 30°C, then an increase in AT increases the output current since the temperature difference between the PV module and the atmospheric is less due to that heat loss is small [33].

5.2 PV module voltage variation with input parameters

Figures 8 (c), and (d) depicts the effects of SF, MT, and AT on the output voltage of the PV module by surface plot, and contour plot. Figure 8 (c) shows that if the SF increases, the PV module output voltage increases, but increasing in module temperature and AT reduces the output voltage since the increase in module and atmospheric temperature increases the heat losses in the atmosphere which will reduce the output voltage. Figure 8 (d) shows the 2D representation of the effect of MT and AT on the output voltage of the PV module at a fixed value of the solar flux. It has already been explained the increase in atmospheric temperature give a negative effect on the output voltage. An increase in atmospheric temperature after 30°C reduces the output voltage.

5.3 PV module power variation with input parameters

Figures 8 (e) and (f) show the variation of output power with the input variables. Figure 8 (e) and (f) show that if SF increases, the power output increases and reaches a maximum of 1000 W/m^2 and produces power above 4500 W, but enhancement in module temperature and atmospheric temperature both reduce the power output since the increase in the heat losses in the atmosphere. Figure 8 (f) shows that if the atmospheric temperature varies between 25°C to 45°C then the voltage produced by the solar panel is 32 to 34 volts.

5. 4 Solar pump discharge variation with input parameters

Figure 8 (g) and (h) represent the discharge variation with the input parameters of the SP. Figure 8(g) shows that as solar flux increases, discharge increases due to more solar energy reached on the solar panel. The discharge decreases as the module temperature increases since the power produced by the solar panel are reduced.

6. Validation of RSM results with Experimental results

6.1 Experimental Test Rig

An experimental setup is located in the Rohilkhand area at locations 28.36°N and 79.43°E, as shown in Figures 1 & 2 [34] and presented in this paper in Figure 9, the details of different parts of the solar pump are shown in Table 4. All PV modules join each other in series, and the description of solar PV modules is given in Table 5. The PV modules convert the solar energy into DC, which is further converted into AC power by the controller of the pump. The brushless type AC synchronous motor is coupled with the submersible pump to pump water.

Table 4. Solar Pump components and properties

Number of solar panels	**15**
Solar panel power(kW)	5
Size of the pump(kW)	3.73 (AC submersible pump)
Tilt angle	28° N
Solar azimuth angle	0°

Table 5 Specifications of solar plate

Parameters	**Nominal Value**
Nominal Maximum Power	335 W
Max voltage	38.46 V
Max current	8.38 A
Open circuit voltage	45.81 V
Short circuit current	9.1 A
Module Efficiency	17.1%
Cell Material	Polycrystalline Si
Size	1961*991*30 mm
Operating Temperature Range	-40 °C to +80 °C
Temperature Coefficient (PMax)	-0.3676 %/°C
Temperature Coefficient (Voc)	-0.2726 %/°C
Temperature Coefficient (Isc)	0.0237 %/°C
NOCT	47 °C

In this section, the RSM predicted results of responses current, voltage, and power output are used to find out the Solar Panel Efficiency (SPE), Exergy Efficiency (EE),

motor efficiency, and overall efficiency theoretically and validated with experimental results of solar pump setup located in FET MJP Rohilkhand University, Bareilly shown in Figure 9. The RSM predicted results were obtained from the model equations (8), (9), (10), and (11) generated after the regression analysis. The experimental data were collected based on the months throughout the year. The solar flux, cell temperature, and atmospheric temperature were recorded from a pyranometer and thermocouple mounted on solar panels. As a result, solar panel efficiency, exgergetic efficiency, motor efficiency, and overall efficiency have been determined. The RSM predicted and experimental results are shown in Table 8.

Table 8 Variation of RSM predicted results with the experimental results

	Predicted value	**Experimental value**	**Error (%)**
Current	7.88 A	7.58 A	3.8%
Voltage	579.48 V	556.3 V	4%
Power	4617.7285 W	4409.93 W	3.5%
Discharge	12.50 m^3/hr	12.12 m^3/hr	3%
PV module Efficiency	17%	16.5%	3%
Exergetic Efficiency	18%	17.5%	3%
Motor Efficiency	90%	89%	2%
Overall Efficiency	15.3%	14.89%	2.5%
Solar Flux (1000 W/m^2), Module Temperature (20°C), Atmospheric Temperature (34.346°C)			

Figure 10 (a) represents the efficiency of the SP to the time of the day. Figure 10 (a) shows that the SPE is suddenly reduced at noon since the PV module temperature is increased. Figure 10 (b) shows the exergetic efficiency variation to the time of the day. Figure 10 (b) shows that EE depends on the MT, atmospheric temperature, and power produced by the panel. After 12 pm, the exegetic efficiency is drastically reduced due to the increase in the module temperature and reduction of power generated by solar panels [35]. The further exegetic efficiency could be increased by providing external cooling over the SP either by air or water cooling [36]. Figure 11 (a) shows the pump efficiency to the time of the day. Figure 11 (a) indicates that pump efficiency is maximum at 12 pm of the day when the pump will develop the maximum manometric head due to the availability of the maximum solar flux. The maximum efficiency of the motor pump is recorded to be 94%, and the minimum efficiency recorded is less than 19% after 3 pm. Figure 11 (b) represents the overall efficiency variation to the time of the day [37]. The overall efficiency is the multiplication of the SP and pumps efficiency. The maximum overall efficiency recorded was only 13% experimentally, and it is 14% as per the RSM results. Figure 11 The motor efficiency and overall efficiency validation of MATLAB SIMULINK with experimental results.

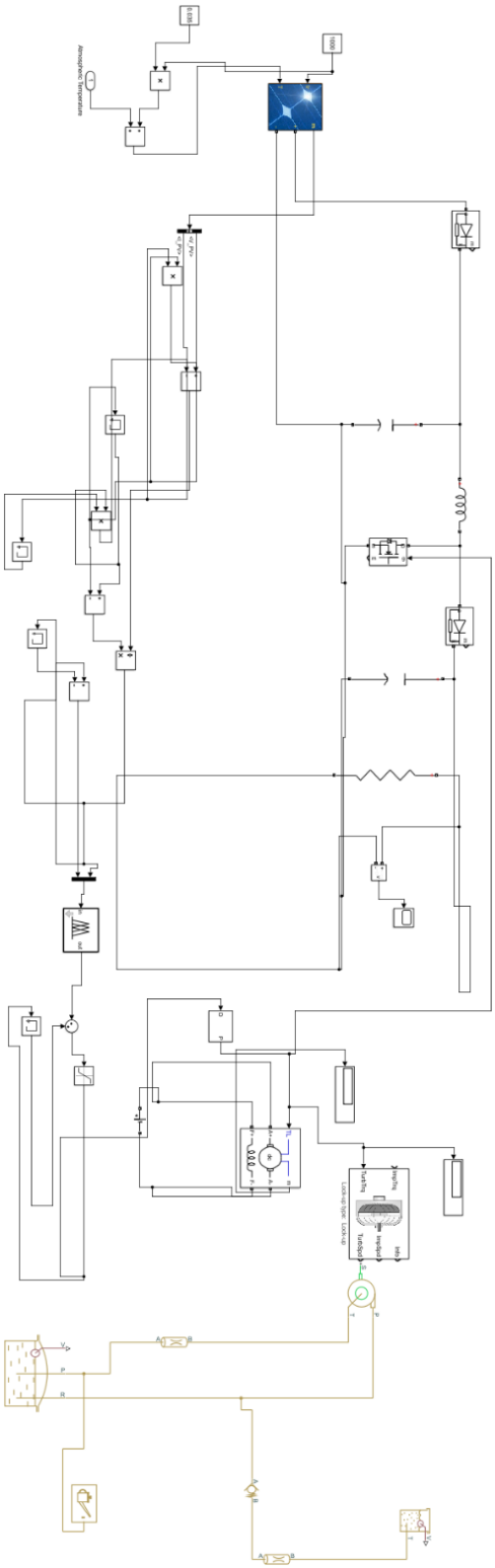

Fig. 2: Solar panel and centrifugal combined circuit diagram with measuring instruments

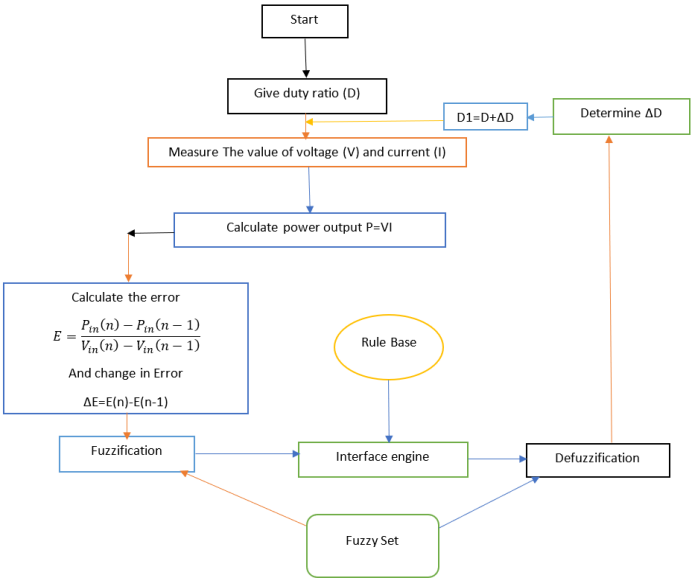

Fig. 3: Fuzzy logic block diagram

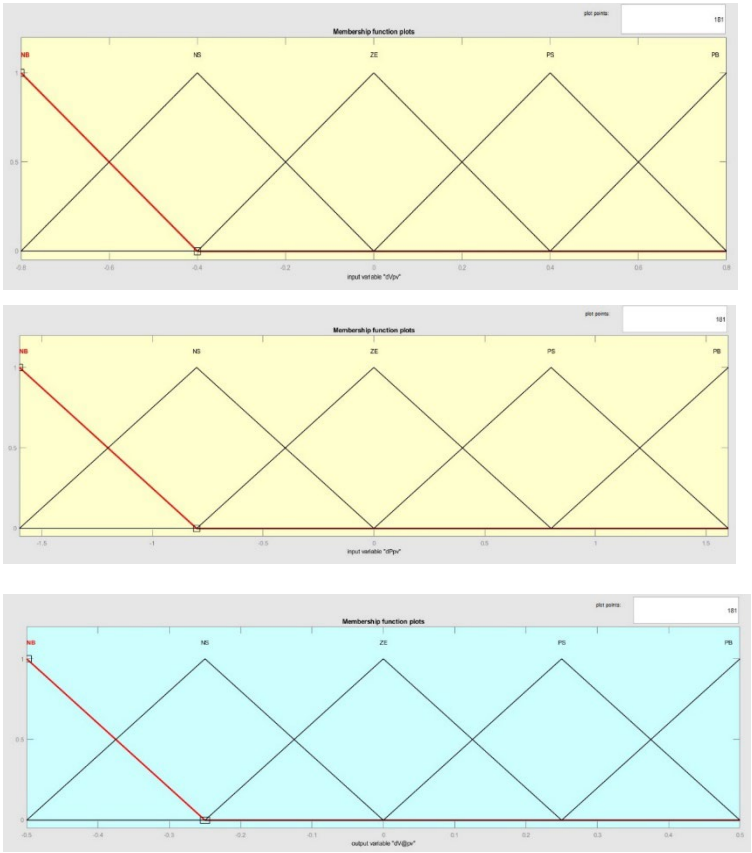

Fig. 4: MF of the two input and one output variables

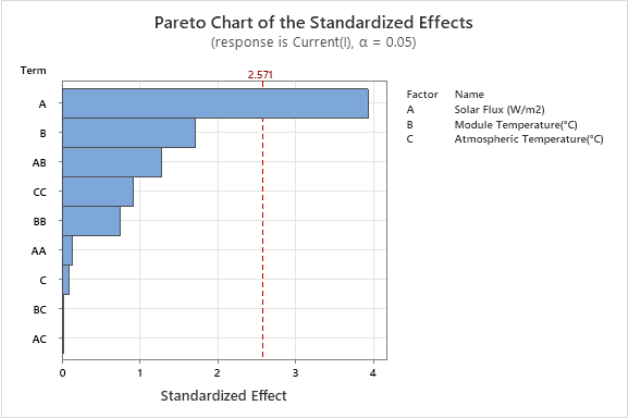

(a)

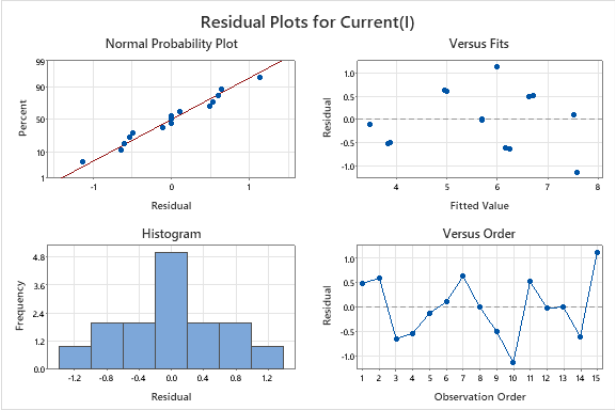

(b)

Fig. 5: Regression model analysis

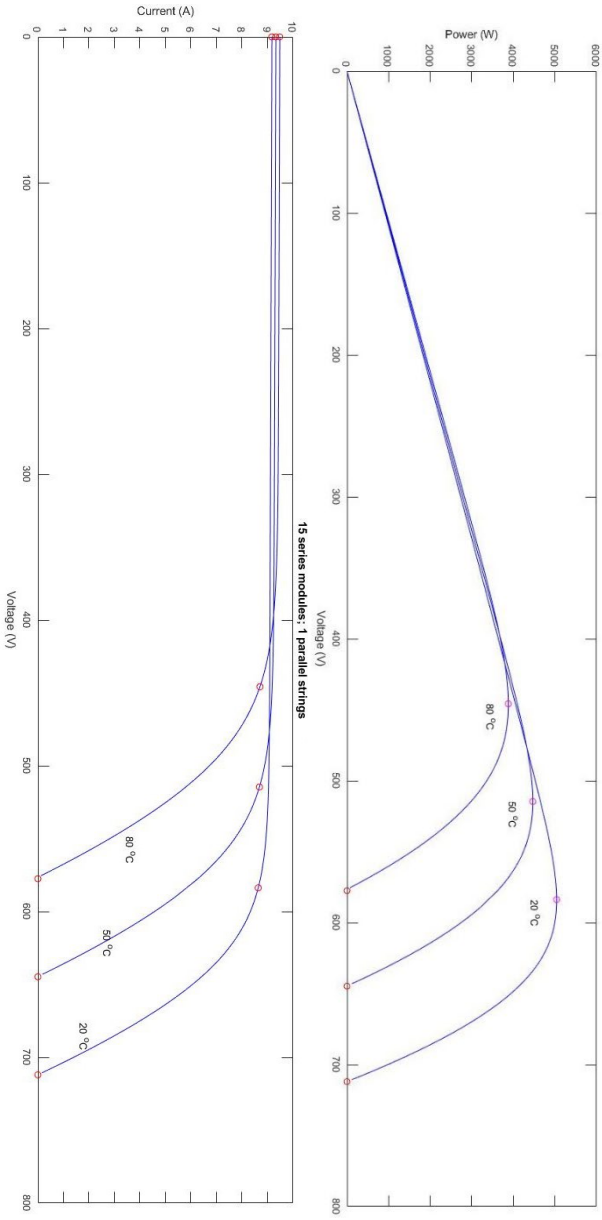

(a) (b)

Fig. 6: current and power output variation of PV module with solar cell temperature

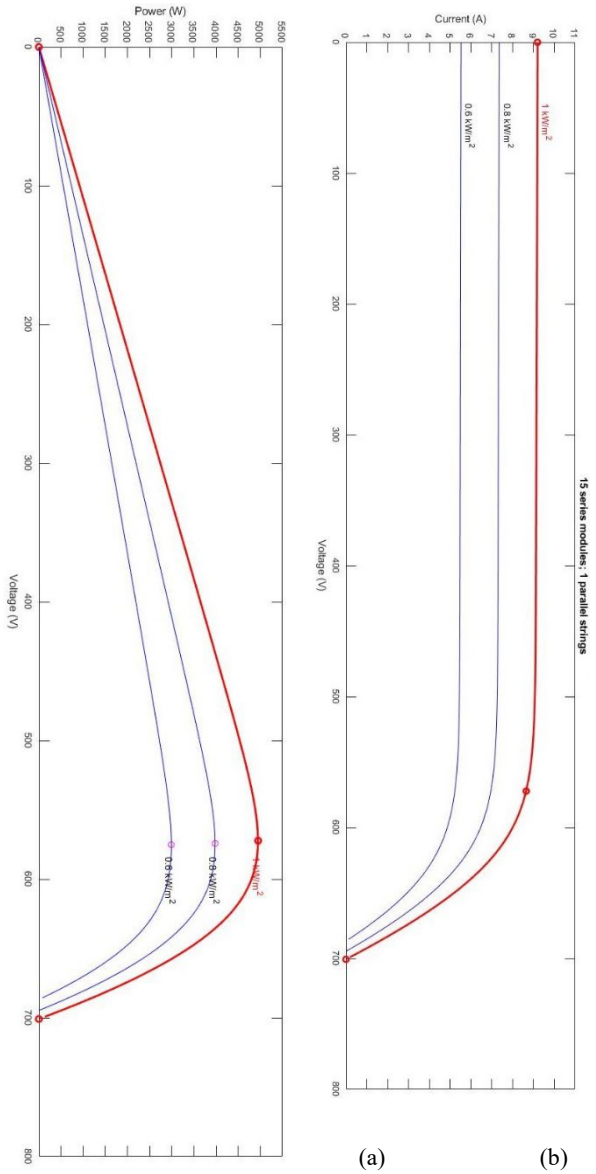

(a) (b)

Fig. 7: current and power output variation of PV module with solar flux

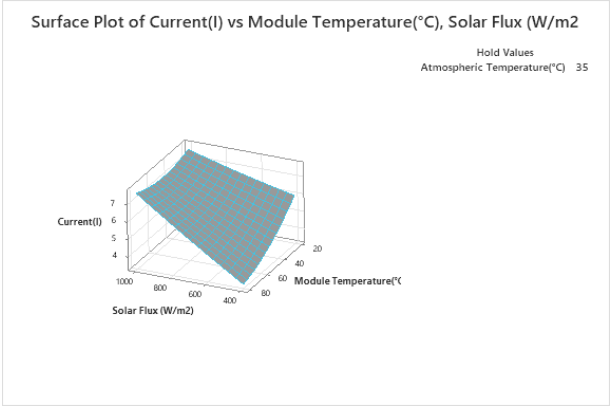

(a) Surface plot of current at 35°C atmospheric temperature

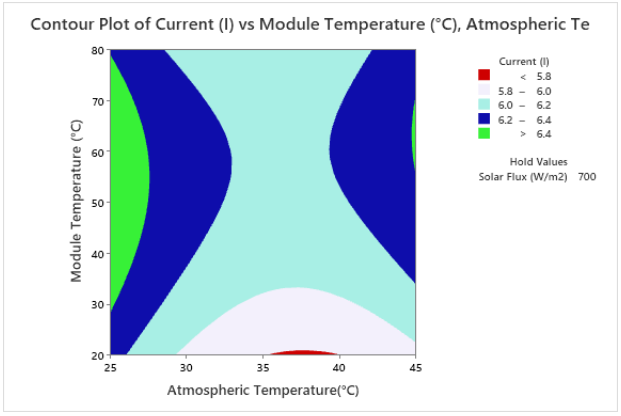

(b) Contour plot of current at 45°C atmospheric temperature

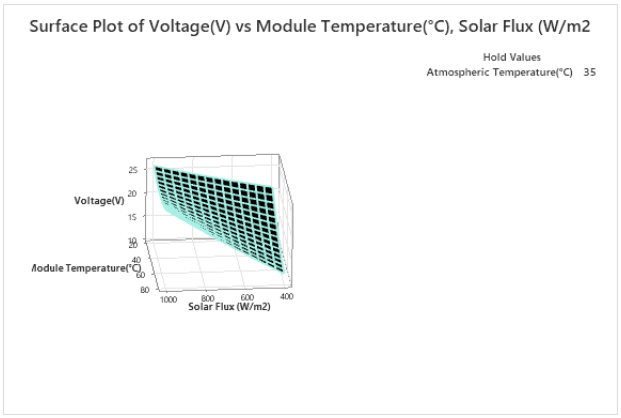

(c) Surface plot of voltage at 45°C atmospheric temperature

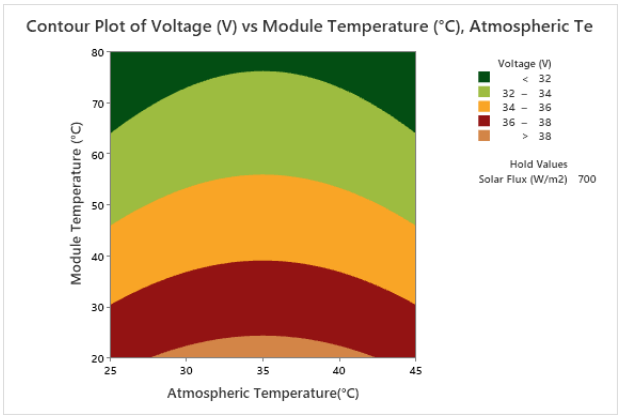

(d) Contour plot of voltage at 45°C atmospheric temperature

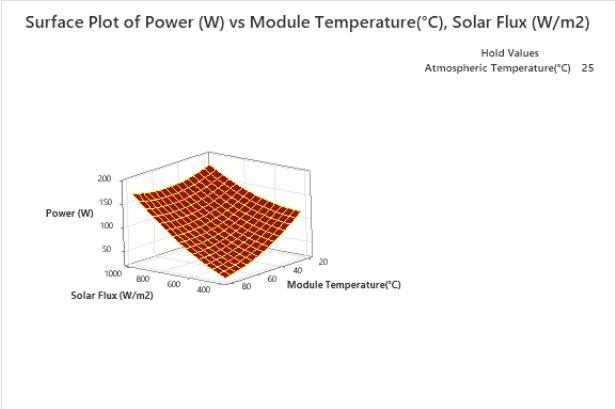

(e) Surface plot of power at 45°C atmospheric temperature

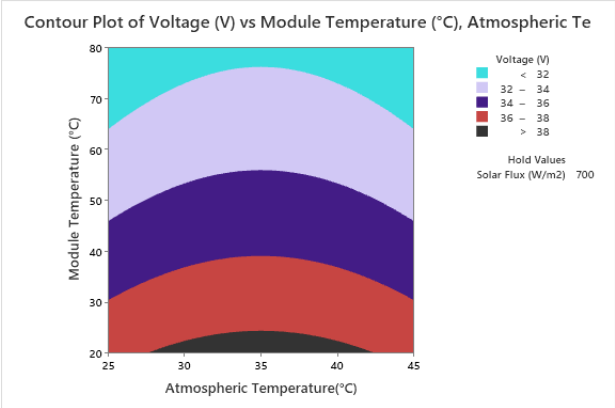

(f) Contour plot of power at 45°C atmospheric temperature

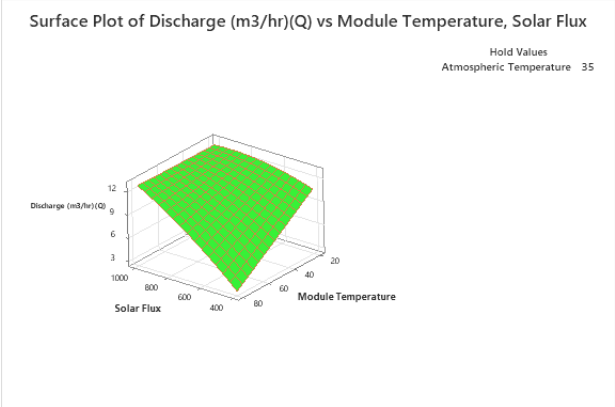

(g) Surface plot of discharge with input variables at constant atmospheric temperature

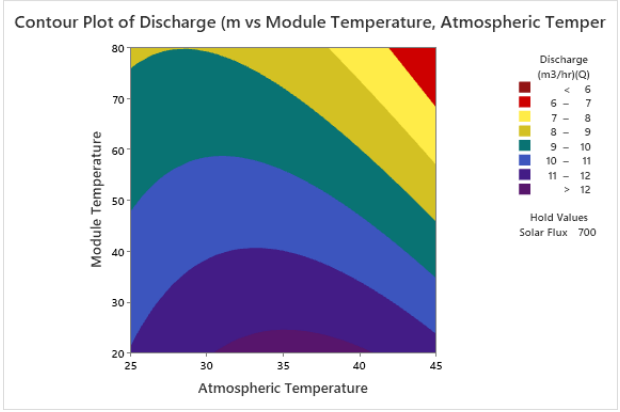

(h) Contour plot of discharge with input variables at constant atmospheric temperature

Fig. 8: Surface and contour plots responses with input variables

Fig. 9: solar panels arrangement

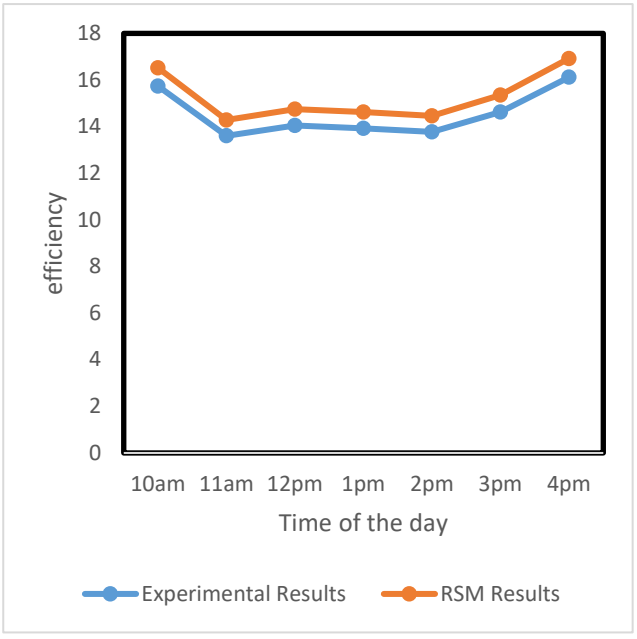

(a) PV module efficiency

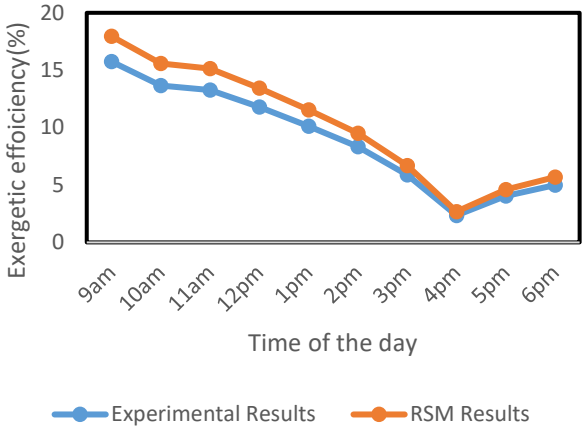

(b) The exergy efficiency of solar panel

Fig.10: PV module efficiency and exergetic efficiency validation of MATLAB SIMULINK results with experimental results

(a) Motor efficiency

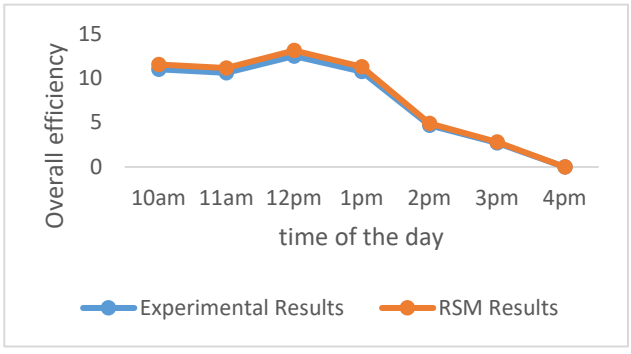

(b) Overall efficiency

Fig. 11 The motor efficiency and overall efficiency validation of MATLAB SIMULINK with experimental results

7. Conclusion

India is located in the tropical region of the world, which has a lot of potential for solar energy. In recent years, a lot of investment in solar power production by PV modules increased due to a lot of atmospheric pollution. In this research paper, a 5 hp power solar pump has been installed in FET MJP Rohilkhand University, Bareilly located at 28.36°N, 79.43°E. The MATLAB Simulink data of output parameters collected at the different settings of input parameters and data generated by model equation have been optimized by the RSM tool of DOE. The Box Benken model was used to design the 3-factor and 3-level trials, then optimized using the commercial tool MINITAB 17 with multiple objective RSM response optimization. The following outcomes were made through the experimental investigation:

- The regression analysis contributed to finding the significant parameters that had the largest impact on the output characteristics, and the DoE based on RSM was precious in planning the experiment. This DoE compacted the time by reducing the number of tests required and represented all data using statistically established models.
- Based on the optimization by RSM, it is concluded that the optimum value of input parameters is module temperature (20°C), atmospheric temperature (34.25°C), and solar flux (1000 W/m^2).
- On the optimum setting of input parameters, the values of the response are maximum current (7.523 amp), maximum voltage (26.16 V), maximum power (196.98 W), and discharge (13.16 m^3/hr), respectively.
- The desirability effect of this model was obtained at 97.07%. In addition, all of the produced regression models for current, voltage, and power output were statistically significant at the 95% confidence level.
- The ANOVA study revealed that the equivalent values of R^2 (81.16%, 81.30%, 80.33%, for current, voltage, and power output, respectively, and adjusted R^2 in the current model suggests that the present proposed model could be effectively matched with the experimental outcomes.
- The use of Fuzzy Logi improves the effectiveness of the Simulink results and minimizes the uncertainty [38].

Acknowledgments

This work was supported by the collaborative project scheme (CRS) fund under the NATIONAL PROJECT IMPLEMENTATION UNIT (NPIU) (A Unit of MHRD, Govt. of India for Implementation of World Bank Assisted Projects in Technical Education) [CRS Project ID: 1-5736521897].

Nomenclature

RSM	Response Surface Methodology
DOE	Design of Experiment
SP	Solar Panel
SPE	Solar Panel Efficiency
EE	Exergy Efficiency

MT	Module temperature
AT	Atmospheric Temperature
AP	Absorber Plate
SPV	Solar Photovoltaic
MPPT	Maximum Power Point Tracking
ANOVA	Analysis of Variance
CHTC	Convection Heat Transfer Coefficient
RHTC	Radiation Heat Transfer Coefficient
RV	Response variable
MF	Membership Function
BC	Boltzmann Constant
VRFB	Vanadium Redox Flow Battery
LPM	Litre Per Minute
HOMER	Hybrid Optimization Of Multiple Energy Resources
OCV	Open Circuit Voltage
c_p	specific heat capacity (J kg^{-1} K^{-1})
P	power (W)
I	Current (A)
V	Voltage (Volt)
V_{OC}	Open Circuit Voltage (Volt)
Q	Discharge (m3/hr)
Ta	Atmospheric Temperature (°C)
Tm	Module Temperature (°C)
q	Heat Flux (W/m2)
I_L	Photocurrent (amp)
I_{SH}	Shunt current
I_O	Reverse Saturation Current

Greek symbols

η	efficiency (–)

References

1) A. Hamidat, “Simulation of the performance and cost calculations of the surface pump,” Renew. Energy, vol. 18, no. 3, pp. 383–392, Nov. 1999, doi: 10.1016/S0960-1481(98)00011-1.
2) Q. Kou, S. A. Klein, and W. A. Beckman, “A method for estimating the long-term performance of direct-coupled PV pumping systems,” Sol. Energy, vol. 64, no. 1–3, pp. 33–40, Sep. 1998, doi: 10.1016/S0038-092X(98)00049-8.
3) M. A. Hossain, M. S. Hassan, S. Ahmmed, and M. S. Islam, “Solar pump irrigation system for green agriculture,” Agric. Eng. Int. CIGR J., vol. 16, no. 4, pp. 1–15, Dec. 2014, Accessed: Jan. 22, 2022. [Online]. Available: https://cigrjournal.org/index.php/Ejounral/article/view/2836.
4) S. Mohammed Wazed, B. R. Hughes, D. O’Connor, and J. Kaiser Calautit, “A review of sustainable solar irrigation systems for Sub-Saharan Africa,” Renew. Sustain. Energy Rev., vol. 81, pp. 1206–1225, Jan. 2018, doi: 10.1016/J.RSER.2017.08.039.
5) S. S. Chandel, M. Nagaraju Naik, and R. Chandel, “Review of solar photovoltaic water pumping system technology for irrigation and community drinking water supplies,” Renew. Sustain. Energy Rev., vol. 49, pp. 1084–1099, Sep. 2015, doi: 10.1016/J.RSER.2015.04.083.
6) H. E. Gad, “PERFORMANCE PREDICTION OF A PROPOSED PHOTOVOLTAIC WATER PUMPING SYSTEM AT SOUTH SINAI, EGYPT CLIMATE CONDITIONS.”
7) A. Mokeddem, A. Midoun, D. Kadri, S. Hiadsi, and I. A. Raja, “Performance of a directly-coupled PV water pumping system,” Energy Convers. Manag., vol. 52, no. 10, pp. 3089–3095, 2011, doi: 10.1016/J.ENCONMAN.2011.04.024.
8) M. Benghanem, K. O. Daffallah, and A. Almohammedi, “Estimation of daily flow rate of photovoltaic water pumping systems using solar radiation data,” Results Phys., vol. 8, pp. 949–954, Mar. 2018, doi: 10.1016/J.RINP.2018.01.022.
9) A. A. Setiawan, D. H. Purwanto, D. S. Pamuji, and N. Huda, “Development of a Solar Water Pumping System in Karsts Rural Area Tepus, Gunungkidul through Student Community Services,” Energy Procedia, vol. 47, pp. 7–14, Jan. 2014, doi: 10.1016/J.EGYPRO.2014.01.190.
10) A. Hamidat, B. Benyoucef, and T. Hartani, “Small-scale irrigation with photovoltaic water pumping system in Sahara regions,” Renew. Energy, vol. 28, no. 7, pp. 1081–1096, Jun. 2003, doi: 10.1016/S0960-1481(02)00058-7.
11) A. K. Daud and M. M. Mahmoud, “Solar powered induction motor-driven water pump operating on a desert well, simulation and field tests,” Renew. Energy, vol. 30, no. 5, pp. 701–714, Apr. 2005, doi: 10.1016/J.RENENE.2004.02.016.
12) P. E. Campana, H. Li, J. Zhang, R. Zhang, J. Liu, and J. Yan, “Economic optimization of photovoltaic water pumping systems for irrigation,” Energy Convers. Manag., vol. 95, pp. 32–41, May 2015, doi: 10.1016/J.ENCONMAN.2015.01.066.
13) A. Bhattacharjee, D. K. Mandal, and H. Saha, “Design of an optimized battery energy storage enabled Solar PV Pump for rural irrigation,” 1st IEEE Int. Conf. Power Electron. Intell. Control Energy Syst. ICPEICES 2016, Feb. 2017, doi: 10.1109/ICPEICES.2016.7853237.
14) Z. Glasnovic and J. Margeta, “Optimization of Irrigation with Photovoltaic Pumping System,” Water Resour. Manag. 2006 218, vol. 21, no. 8, pp. 1277–1297, Sep. 2006, doi: 10.1007/S11269-006-9081-8.
15) I. Odeh, Y. G. Yohanis, and B. Norton, “Economic viability of photovoltaic water pumping systems,”

Sol. Energy, vol. 80, no. 7, pp. 850–860, Jul. 2006, doi: 10.1016/J.SOLENER.2005.05.008.
16) M. Jamil, A. Anees, M. R.-A. J. of Electrical, and undefined 2012, "SPV based water pumping system for an academic institution," article.ajepes.org, vol. 1, no. 1, pp. 1–7, 2012, doi: 10.11648/j.epes.20120101.11.
17) R. Foster and A. Cota, "Solar Water Pumping Advances and Comparative Economics," Energy Procedia, vol. 57, pp. 1431–1436, Jan. 2014, doi: 10.1016/J.EGYPRO.2014.10.134.
18) A. Kumar and T. C. Kandpal, "Potential and cost of CO2 emissions mitigation by using solar photovoltaic pumps in India," http://dx.doi.org/10.1080/14786450701679332, vol. 26, no. 3, pp. 159–166, Sep. 2007, doi: 10.1080/14786450701679332.
19) N. M. Kumar, J. Vishnupriyan, and P. Sundaramoorthi, "Techno-economic optimization and real-time comparison of sun tracking photovoltaic system for rural healthcare building," J. Renew. Sustain. Energy, vol. 11, no. 1, p. 015301, Jan. 2019, doi: 10.1063/1.5065366.
20) V. Modi and S. P. Sukhatme, "Estimation of daily total and diffuse insolation in India from weather data," Sol. Energy, vol. 22, no. 5, pp. 407–411, Jan. 1979, doi: 10.1016/0038-092X(79)90169-5.
21) L. A. Zadeh, "Fuzzy sets," Inf. Control, vol. 8, no. 3, pp. 338–353, 1965, doi: 10.1016/S0019-9958(65)90241-X.
22) F. A. O. Aashoor and F. V. P. Robinson, "Maximum power point tracking of photovoltaic water pumping system using fuzzy logic controller," Proc. Univ. Power Eng. Conf., 2013, doi: 10.1109/UPEC.2013.6714969.
23) G. Li, Y. Jin, M. W. Akram, and X. Chen, "Research and current status of the solar photovoltaic water pumping system – A review," Renew. Sustain. Energy Rev., vol. 79, no. December 2016, pp. 440–458, 2017, doi: 10.1016/j.rser.2017.05.055.
24) P. K. S. Rathore, S. S. Das, and D. S. Chauhan, "Perspectives of solar photovoltaic water pumping for irrigation in India," Energy Strateg. Rev., vol. 22, no. October, pp. 385–395, 2018, doi: 10.1016/j.esr.2018.10.009.
25) H. Fayaz, R. Nasrin, N. A. Rahim, and M. Hasanuzzaman, "Energy and exergy analysis of the PVT system: Effect of nanofluid flow rate," Sol. Energy, vol. 169, pp. 217–230, Jul. 2018, doi: 10.1016/J.SOLENER.2018.05.004.
26) V. Karthikeyan, C. Sirisamphanwong, S. Sukchai, S. K. Sahoo, and T. Wongwuttanasatian, "Reducing PV module temperature with radiation based PV module incorporating composite phase change material," J. Energy Storage, vol. 29, p. 101346, Jun. 2020, doi: 10.1016/J.EST.2020.101346.
27) A. Maleki, P. T. T. Ngo, and M. I. Shahrestani, "Energy and exergy analysis of a PV module cooled by an active cooling approach," J. Therm. Anal. Calorim., vol. 141, no. 6, pp. 2475–2485, Sep. 2020, doi: 10.1007/S10973-020-09916-0.
28) E. Radziemska, "The effect of temperature on the power drop in crystalline silicon solar cells," Renew. Energy, vol. 28, no. 1, pp. 1–12, Jan. 2003, doi: 10.1016/S0960-1481(02)00015-0.
29) S. Dubey, J. N. Sarvaiya, and B. Seshadri, "Temperature Dependent Photovoltaic (PV) Efficiency and Its Effect on PV Production in the World – A Review," Energy Procedia, vol. 33, pp. 311–321, Jan. 2013, doi: 10.1016/J.EGYPRO.2013.05.072.
30) A. A. S. Esmeail, S. Oncu, and N. Altin, "An MPPT Controlled Three Phase PV Supplied Water Pumping System," Proc. 13th Int. Conf. Electron. Comput. Artif. Intell. ECAI 2021, Jul. 2021, doi: 10.1109/ECAI52376.2021.9515018.
31) E. M. Salilih, Y. T. Birhane, and S. H. Arshi, "Performance analysis of DC type variable speed solar pumping system under various pumping heads," Sol. Energy, vol. 208, pp. 1039–1047, Sep. 2020, doi: 10.1016/J.SOLENER.2020.08.071.
32) N. Mousavi, G. Kothapalli, D. Habibi, S. W. Lachowicz, and V. Moghaddam, "A real-time energy management strategy for pumped hydro storage systems in farmhouses," J. Energy Storage, vol. 32, no. September, p. 101928, 2020, doi: 10.1016/j.est.2020.101928.
33) B. S. Pali and S. Vadhera, "Uninterrupted sustainable power generation at constant voltage using solar photovoltaic with pumped storage," Sustain. Energy Technol. Assessments, vol. 42, no. November, p. 100890, 2020, doi: 10.1016/j.seta.2020.100890.
34) V. Singh and V. S. Yadav, "Application of RSM to Optimize Solar Pump LCOE and Power Output,"https://doi.org/10.1080/03772063.2022.2069165, pp. 1–12, May 2022, doi: 10.1080/03772063.2022.2069165.
35) A. Maleki, P. T. T. Ngo, and M. I. Shahrestani, "Energy and exergy analysis of a PV module cooled by an active cooling approach," J. Therm. Anal. Calorim. 2020 1416, vol. 141, no. 6, pp. 2475–2485, Jul. 2020, doi: 10.1007/S10973-020-09916-0.
36) S. Choudhary, A. Sharma, S. Gupta, H. Purohit, and S. Sachan, "Use of RSM technology for the optimization of received signal strength for LTE signals under the influence of varying atmospheric conditions," Evergr. Jt. J. Nov. Carbon Resour. Sci. Green Asia Strateg., vol. 07, pp. 500–509, 2020, doi: 10.5109/4150469.
37) Y. Gunawan, V. Nurliyanti, N Akhiriyanto, S kasbi, "A comparative study of photovoltaic water pumping -Driving Conventional AC single phaseand three phase motor submersible pumps", Evergr. Jt. J. Nov.

Carbon Resour. Sci. Green Asia Strateg., vol. 09, pp. 893-902, 2022, doi: https://doi.org/10.5109/4843121.

38) Laxmi Kant Sagar and D Bhagwan Das (2022) 'Fuzzy Expert System for Determining State of Solar Photo Voltaic Power Plant Based on Real-Time Data', Evergreen, 9(3), pp. 870–880. doi: 10.5109/4843118.